Title: Impaired thalamic burst firing in Fragile X syndrome

Authors: Ronan T. O'Shea[1,2,3], Nicholas J. Priebe[1,2,3,5], Darrin H. Brager[4,5,6]

[1]Center for Perceptual Systems
[2]Center for Learning and Memory
[3]Department of Neuroscience, The University of Texas at Austin, Austin, Texas, 78712, USA
[4]Department of Life Sciences, University of Nevada, Las Vegas, Las Vegas, Nevada, 89154, USA
[5]Senior authors
[6]Corresponding author

Abstract

Burst and tonic firing modes in the thalamic relay cells underlie the selective and flexible relay of sensory information to cortex, a capacity which is dysregulated in Fragile X syndrome (FX). Here we show that relay cell bursting is impaired in FX mutant mice. The voltage sensitivity for Ca^{2+}-dependent spikes, which underlie bursting, is hyperpolarized in the FX relay cells, contributing to reduced burst frequency and duration in FX syndrome.

Results

In mammals, sensory information is relayed from the periphery to the neocortex via the thalamus. While the thalamus is often considered a relay station, it also acts as a critical gate of information: the statistics of sensory inputs and modulatory feedback from neocortex and brainstem alter how the thalamus conveys sensory information to the neocortex[1]. These inputs shift thalamic relay cells between two modes of firing: burst and tonic modes[2]. Bursting is mediated by the generation of the low threshold spike (LTS), a non-linear depolarization of membrane potential mediated by T-type Ca^{2+} channels[3–6].

Burst and tonic firing play complementary roles in relaying sensory information. Burst mode, in which relay cells fire a series of action potentials (APs) with short inter-spike intervals (ISIs), gates sensory information flow by transmitting brief, spatiotemporally restricted drive to the neocortex[7–9]. Tonic mode, with spike timing characterized by Poisson statistics, passes peripheral sensory drive in a linear manner. Burst mode modulates the information relayed to neocortex, as a burst of APs encode three times as much information as tonic APs[10]. Bursts are hypothesized to perform a "wake-up call" to activate cortical targets more than single, tonic spikes, following a period of inactivity[11,12].

We hypothesized that a disruption of thalamic relay dynamics contributes to dysregulated sensory processing in autism spectrum disorders (ASD). This hypothesis is consistent with the observation that while psychophysical measures of sensitivity among people with ASD are normal, these subjects often struggle to segment task relevant sensory inputs from noise [13–18]. In addition, ASD is associated with both hyper- and hyposensitivity across sensory modalities[19–22]. Taken together, these symptoms point to an alteration in how sensory information is gated. Because sensory information across modalities flows through the thalamus to reach the neocortex, an impairment in thalamic relay cell dynamics should alter information gating. To test our hypothesis, we compared thalamic population activity in wild type (WT) and FMR1-knockout (FX) mice, a common experimental model for exploring the physiological basis of the autistic phenotype[23].

To compare the distributions of thalamic firing patterns in WT and FX mice, we densely sampled single unit activity in LGN of awake WT and FX mice with the

Neuropixels 1.0 probe[24]. We classify a spike as emerging from burst or tonic firing mechanisms by the preceding and subsequent ISI. The first AP in a burst is preceded by at least 100ms of silence, followed by APs separated by less than 4ms; ending with an ISI longer than 4ms (Fig. 1a, green boxes)[25]. All other spikes are classified as tonic. The pattern of tonic and burst spiking is consistent across WT relay cells (Fig. 1a). In contrast, relay cells in FX LGN fired primarily in the tonic mode (Fig. 1b). The frequency of burst events was significantly lower in FX than WT populations during both spontaneous and visually-evoked activity (Fig. 2a, left). Even when FX relay cells did burst, the bursts contained significantly fewer APs compared to bursts from WT relay cells (Fig 2c).

WT relay cells also had higher baseline firing rates than FX relay cells (Fig. 2a, right). This difference in baseline firing rate could underlie the difference in burst frequency which we observe between the genotypes. To explore this possibility, we resampled our WT dataset to create a sample with firing rate statistics matched to the FX dataset (Fig. 2b, right). The distribution of burst frequencies for the resampled WT population remained significantly higher than that of the FX population, indicating that the disruption of thalamic firing dynamics in FX cannot be explained simply by a difference in the baseline firing rate of neurons across genotypes (Fig. 2b, left). These differences in thalamic firing dynamics between genotypes could also not be explained by differences in locomotion, as WT and FX mice spent equal amounts of time running during recordings.

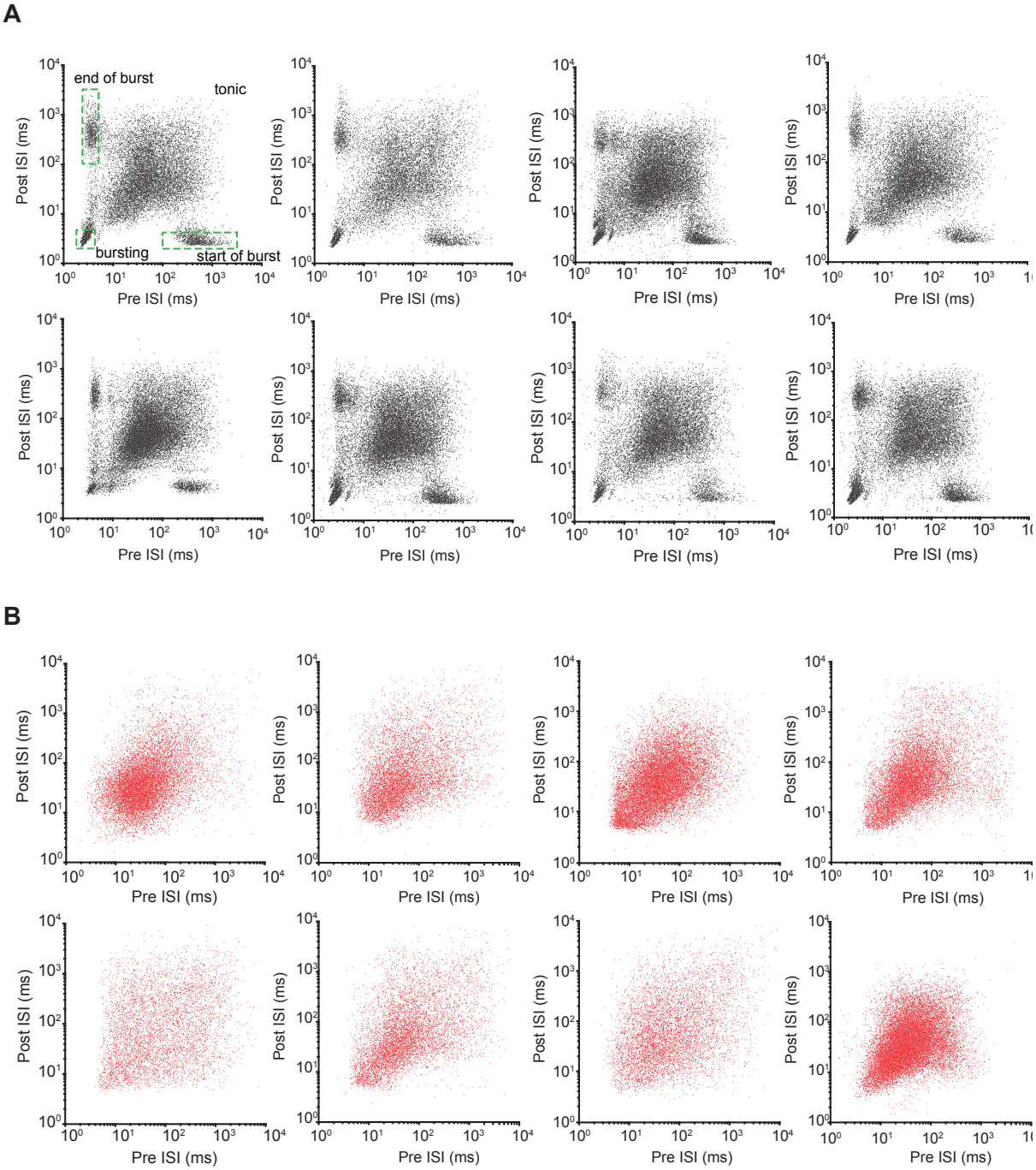

Figure 1: **Example ISI plots for LGN single units. a**. Example WT LGN ISI distributions, where each scatter point represents the pre and post ISI for a single spike. Green boxes indicate the criteria for spikes being classified as part of a burst. **b**. As in **a**, for example FX LGN single units.

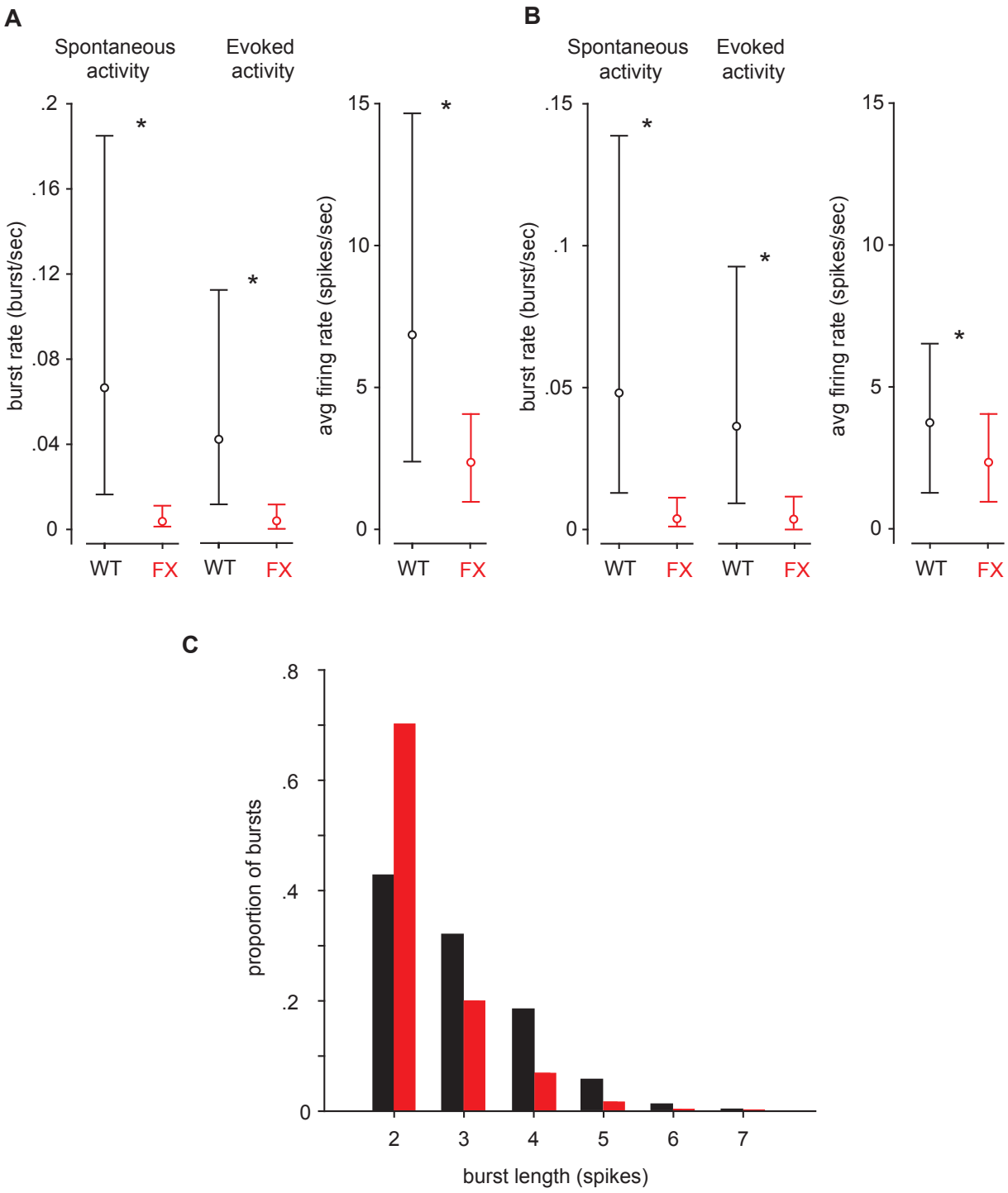

Figure 2: Burst firing statistics across WT and FX LGN populations: a. (Left) Distribution of burst rates for WT (black) and FX (red) populations. (WT spontaneous mean=.16 +/- .25 bursts/sec, median=.07 bursts/sec; FX spontaneous mean=.01+/- .03 bursts/sec, median=.004 bursts/sec; WT evoked mean=.09+/- .11 bursts/sec, median=.04 bursts/sec; FX evoked mean=.01+/- .03 bursts/sec, median=.004 bursts/sec) (Right) Distributions of baseline firing rates (WT mean=10.3 +/- 10.4 spikes/sec, median=6.9; 3.2

+/-3.3 spikes/sec, median=2.4 spikes/sec). Circles are the medians of the distributions. Lower and upper bars indicate the 25th and 75th percentiles of the distributions, respectively. *: p<.01 for a Wilcoxon rank sum test between FX and WT population data. **b**. As in **a**, for the resampled WT dataset. (WT resampled spontaneous mean=.13 +/- .19 bursts/sec, median=.05 bursts/sec; WT resampled evoked mean=.07+/- .10 bursts/sec, median=.04 bursts/sec) (WT resampled baseline firing rate mean=4.6 +/- 4.1 spikes/sec, median=3.7 spikes/sec) **c**. Histogram of the number of spikes in each burst across the WT and FX LGN populations (FX mean= 2.46 +/-.81 spikes/burst, WT mean= 2.94 +/- 1.02 spikes/burst).

One potential mechanistic explanation for impaired bursting in FX LGN is that the function of voltage gated T-type Ca^{2+} channels, which switch thalamic relay cells to burst mode at hyperpolarized membrane potentials, is altered in FX [3,4,26–28]. To examine this possibility, we performed *in vitro* electrophysiological recordings from thalamic neurons in WT and FX mice. Whole cell recordings were made from neurons in both the LGN and medial dorsal thalamus and all results reported were consistent across these two nuclei. Both WT and FX neurons showed an increase in AP firing rate in response to depolarizing current injections (Fig. 3a). WT neurons however, fired fewer APs compared to FX neurons particularly at the smaller current injections (Fig. 3b, mixed-factor ANOVA, interaction between genotype and amplitude: $F(11,195) = 3.818$, $p < 0.0001$). At larger current injections, firing rate increased as a linear function of current amplitude, in line with the observation from *in vivo* recordings that the tonic mode represents a linear relay of sensory inputs[2]. When neurons were held at -60 mV (near the resting V_m) however, WT neurons reliably fired a burst of APs in response to small, brief current injections (Fig. 3c). In the burst mode these neurons integrated inputs in a nonlinear manner, as increasing the duration of the current step up to 3000ms did not elicit more spikes after the initial burst, consistent with the proposed gating function of burst spiking. In contrast, FX neurons fired in the tonic mode and increased the number

of spikes fired with increasing current duration (Fig. 3c, d; mixed-factor ANOVA, interaction between genotype and duration: $F(5,80) = 8.193$, $p < 0.0001$). At rest, WT thalamic neurons respond to excitatory drive in the burst mode, amplifying sensory drive

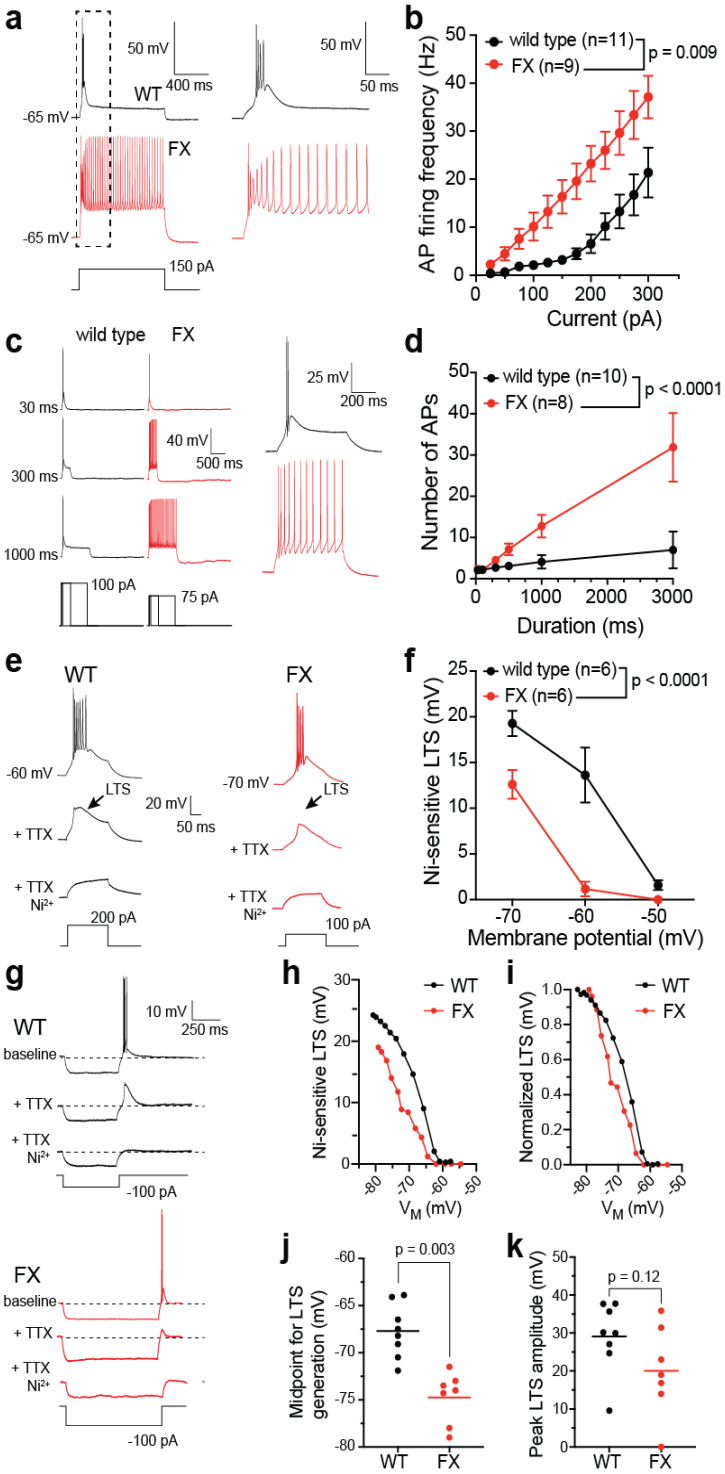

Figure 3: Hyperpolarization of LTS generation. a. AP firing recorded from single thalamic neuron in response to current injection. Dashed box shows initial action potentials expanded at right. **b.** FX thalamic neurons fire more APs compared to WT. **c.** AP firing in response to current injections of variable duration. **d.** FX neurons show a linear increase in firing frequency consistent with tonic firing mode while WT thalamic neurons fire a brief train of 2-3 APs consistent with burst firing mode. **e.** Representative traces showing a burst of AP, isolation of the LTS by TTX, and block of the LTS by Ni^{2+} **f.** Summary plot showing that LTS initiation is hyperpolarized in FX thalamic neurons. **g.** Example traces showing a rebound burst of APs following hyperpolarization, isolation of the LTS, and block of the LTS in WT and FX neurons. **h,i.** Individual WT and FX neurons showing raw (h) and normalized (i) LTS amplitude as a function of steady-state V_M. **j.** Midpoint of LTS generation is hyperpolarized in FX compared to WT thalamic neurons. **k**, LTS amplitude between FX and WT thalamic neurons.

following a period of inactivity, whereas FX thalamic neurons respond to same excitatory drive in tonic mode[7,11]. There were no differences in the passive or AP properties between WT and FX neurons suggesting that the differences in burst firing were not likely due to Na^+ or K^+ channel dependent mechanisms (Supplementary Table 1).

The lack of bursts in FX relay cells at rest could be due to an absence of the LTS altogether, or a change in its voltage-dependence. We delivered a depolarizing current step, in the presence of 1 μM TTX to block Na^+-dependent APs, from a series of membrane potentials and measured the LTS. We found that the LTS was generated in FX relay cells, but only at a more hyperpolarized V_M. While the LTS in WT relay cells was apparent at -60 mV, the LTS in FX relay cells only began to emerge at -70 mV (Fig. 3e-f; mixed-factor ANOVA, interaction between genotype and V_M: $F(2,20) = 8.958$, $p = 0.0017$). Even when the LTS was evoked, the amplitude was significantly smaller in FX neurons compared to WT (FX mean= 12.6 +/- 3.8 mV, WT mean= 19.3 +/- 3.4 mV). We examined in detail the altered voltage dependence of the LTS in FX mice by measuring the LTS that follows hyperpolarizing current steps from a holding potential of -55 mV (Fig. 3g). In agreement with the experiment above, the voltage sensitivity of the rebound LTS was hyperpolarized in FX thalamic neurons compared to WT (Fig. 3h-j; unpaired t-test, $t=4.880$, $df = 13$, $p = 0.0003$). To confirm the contribution of T-type Ca^{2+} channels to the LTS, at the conclusion of the LTS recordings, 50 μM Ni^{2+}, a blocker of the T-type Ca^{2+} channels, was added to the extracellular saline (Fig. 3e)[29].

These *in vitro* results provide a mechanistic basis for the dramatic reduction in burst frequency and duration FX LGN *in vivo*. While the LTS remains in FX relay cells, it

requires greater membrane potential hyperpolarization for activation, which may only rarely occur *in vivo*. A smaller LTS when FX cells do transition to burst mode means less activation of voltage-dependent Na^+ channels for driving APs, which will reduce the number of spikes in a burst.

There are additional mechanisms which may account for the functional disruption of bursts in FX LGN. Modulatory inputs to the LGN from brainstem cholinergic projections or thalamic reticular nucleus GABAergic projections could be altered in FX[30,31]. Properties of the retinal drive to the LGN which can evoke bursting could also be altered in FX mice[32]. These explanations are not mutually exclusive, as disruptions at both the network and cellular levels could contribute to the observed changes in thalamic firing dynamics *in vivo*.

Our findings indicate that neural mechanisms within the thalamus responsible for dynamically filtering sensory input are impaired in Fragile X syndrome. This disruption could impair the downstream cortical processing of sensory information, and the overall ability to detect, attend to, and to interpret salient stimuli. As the thalamus is the gateway to the neocortex across sensory modalities, we suggest that this alteration could be linked to the hypo- and hypersensitivities to the environment commonly experienced by people with ASD. Our observations suggest that restoring the normal voltage-dependence of T-type Ca^{2+} channels could be a therapeutic target for people with ASD experiencing altered sensitivity to complex sensory environments.

Methods

In vivo extracellular recordings

All experiments were approved by the University of Texas at Austin's Institutional Animal Care and Use Committee, which maintains Association for Assessment and Accreditation of Laboratory Animal Care accreditation. All methods were carried out in accordance with relevant guidelines and regulations.

Animal preparation

Electrophysiology experiments were conducted using adult (P35 and older) C57/BL6J mice (WT) (Jackson Labs #000664) of both sexes (n = 11) and FMR1 knockout mice (FX) (Jackson Labs #003025) of both sexes (n=6), all housed on a 12-hour light-dark cycle.

For all surgical procedures, mice were anesthetized with isoflurane (2.5% induction, 1%–1.5% surgery) and given two preoperative subcutaneous injections of analgesia (5 mg/kg carprofen, 3.5 mg/kg Ethiqa) and anti-inflammatory agent (dexamethasone, 1%). Mice were kept warm with a water-regulated pump pad. Each mouse underwent two surgical procedures. The first was the mounting of a metal frame over the visual cortex using dental acrylic, used for head fixation of the mouse during experiments. The second was a 1-2mm diameter craniotomy centered 2.5mm posterior of bregma and 2mm lateral of midline in the right hemisphere followed by a durotomy. Exposed brain tissue was preserved prior to experiments with KWIK-SIL silicone adhesive (World Precision Instruments). Surgical procedures were always performed on a separate day from electrophysiological recordings.

Electrophysiology

During all experiments, mice were awake, head restrained, and moved freely on a custom-built wheel. Mice were habituated to handling and head restraint over 1 week following recovery from the craniotomy in sessions increasing from 15 minutes to 1 hour. The axle of the wheel was connected to a quadrature encoder to track locomotion during the experiment.

LGN recordings were made using a Neuropixels 1.0 probe implanted acutely 2500 μm posterior of bregma and 2000 μm lateral of midline and lowered to 2500-3200 μm depth. The electrode tip was lowered to the ventral extent of the LGN as identified by clearly evoked visual responses in the neural activity. Raw traces were acquired at 30 kHz using the spikeGLX System.

Putative single units were isolated from the raw traces offline using Kilosort3[33]. We conducted further manual sorting of single units using the Phy GUI (https://github.com/cortex-lab/phy). All subsequent analysis of single unit spiking data was performed using custom MATLAB code.

Each spike from a single unit was defined as arising from the burst or tonic firing mode based on the pre and post ISI. The first AP in a burst is preceded by at least 100ms of silence, followed by APs separated by less than 4ms. A burst ends with an ISI greater than 4ms. In our data, as reported previously, the end of a burst tended to be followed by a period of at least 100ms of silence[25]. All spikes not meeting these criteria for bursting were classified as tonic spikes.

Visual Stimuli

A monochrome LED projector by Texas Instruments (Keynote Photonics) with spectral peak at 525 nm was used to generate stimuli with a 60Hz refresh rate onto a Teflon screen which provides a near-Lambertian surface[34]. The screen was 12.5 cm high x 32 cm wide, equating to approximately 64° x 116° of visual angle. Stimuli were coded using the Psychophysics Toolbox extension in MATLAB.

Drifting gratings were presented at a spatial frequency of .02 cycles/degree, and a temporal frequency of 2 Hz, drifting at 0, 45, 90, 135 degrees, for 50 repeats of each stimulus. Each grating was preceded and followed by 1 second of a blank screen at uniform luminance. 50 repeats of 10 second natural movies were also presented with each repeat followed by a 6 second blank screen at uniform luminance. Movie 1 consisted of honeybees flying in a garden (Ian Nauhaus, UT Austin) and Movie 2 consisted of monkeys playing in snow (David Leopold, NIMH).

In vitro whole-cell recordings

All experiments were approved by the University of Nevada, Las Vegas and the University of Texas at Austin Institutional Animal Care and Use Committees, which maintain Association for Assessment and Accreditation of Laboratory Animal Care accreditation. All methods were carried out in accordance with relevant guidelines and regulations.

Acute slice preparation

Brain slices containing either the medial dorsal or visual thalamus were prepared and maintained as in prior studies[35,36]. Briefly, mice had free access to food and water and were housed in a reverse light-dark cycle of 12 hr on/ 12 hr off. Experiments used male 2–4-month-old wild type and *fmr1* knockout (FX) mice on a C57/Bl6 background

(JAX: strain #000664). Mice were anesthetized using a ketamine/xylazine cocktail (100/10 mg/kg) and then underwent cardiac perfusions with ice-cold saline consisting of (in mM): 2.5 KCl, 1.25 NaH_2PO_4, 25 $NaHCO_3$, 0.5 $CaCl_2$, 7 $MgCl_2$, 7 dextrose, 205 sucrose, 1.3 ascorbic acid, and 3 sodium pyruvate (bubbled constantly with 95% O_2/5% CO_2 to maintain pH at ~7.4). The brain was removed and sliced into 300 μM coronal (for MD) or parasagittal (for LGN) sections using a vibrating tissue slicer (Vibratome 300, Vibratome Inc). The slices were placed in a chamber filled with artificial cerebral spinal fluid (aCSF) consisting of (in mM): 125 NaCl, 2.5 KCl, 1.25 NaH_2PO_4, 25 $NaHCO_3$, 2 $CaCl_2$, 2 $MgCl_2$, 10 dextrose, 1.3 ascorbic acid and 3 sodium pyruvate (bubbled constantly with 95% O_2/5% CO_2) for 30 minutes at 35°C and then held at room temperature until time of recording.

In vitro electrophysiology

Slices were placed individually, as needed, into a submerged recording chamber, continuously perfused with oxygenated extracellular saline containing (in mM): 125 NaCl, 3 KCl, 1.25 NaH_2PO4, 25 $NaHCO_3$, 2.0 $CaCl_2$, 1.0 $MgCl_2$, and 21 dextrose (pH 7.4) at 32-34°C. LGN and MD cells were viewed with a 60x water immersion objective and Dodt contrast. Ionotropic glutamatergic and GABAergic synaptic transmission were blocked with 20 μM DNQX, 25 μM D-AP5, and 2 μM gabazine. Current clamp recordings were made using a Dagan BVC-700 amplifier and acquisition software Axograph X (Axograph) or SutterPatch (Sutter). Data were sampled at 20-50 kHz, filtered at 3 kHz, and then digitized by either an InstruTECH ITC-18 interface (HEKA) or Dendrite interface (Sutter). The internal recording solution consisted of (in mM): 135 K-gluconate, 10 HEPES, 7 NaCl, 7 K_2-phosphocreatine, 0.3 Na-GTP, 4 Mg-ATP (pH

corrected to 7.3 with KOH). Recording pipettes had a resistance of 4-6 MΩ when filled with the pipette solution. During current clamp recordings, series resistance was monitored throughout, and the experiment was discarded if it exceeded 30 MΩ or varied by >20%. The LTS was isolated by blocking Na^+-dependent APs with TTX (1 μM) during whole-cell recordings. Following LTS recordings, $NiCl_2$ (50 μM) was applied to confirm that the measured LTS was mediated by T-type Ca^{2+}channels[29].

Supplementary Table 1: Neuronal Properties

	wild type	Fmr1 KO	p-value	n
Passive Properties				
Resting V_M (mV)	-59.3 ± 1.89	-58.6 ± 2.39	0.8262	11, 9
Input resistance (MΩ)	111.3 ± 14.49	129.1 ± 15.16	0.2541	11, 9
τ_M (ms)	21.1 ± 3.62	27.7 ± 3.42	0.232	6, 6
Voltage sag (%)	13.6 ± 3.66	13 ± 4.52	0.92	7, 6
Active Properties				
AP threshold (mV)	-38.5 ± 2.77	-37.4 ± 3.19	0.8003	8, 6
AP amplitude (mV)	81.8 ± 3.35	81.5 ± 4.53	0.9414	8, 6
AP width (μs)	698 ± 23.4	771 ± 65.8	0.2606	8, 6
AP maximum rate of rise (mV/ms)	269 ± 16.4	278 ± 33.2	0.8099	8, 6
AP maximum rate of fall (mV/ms)	-122 ± 5.9	-107 ± 9.8	0.1817	8, 6

Works Cited

1. Usrey, W. M. & Sherman, S. M. Corticofugal circuits: Communication lines from the cortex to the rest of the brain. *J Comp Neurol* **527**, 640–650 (2019).
2. Sherman, S. M. Tonic and burst firing: dual modes of thalamocortical relay. *Trends in Neurosciences* **24**, 122–126 (2001).
3. Jahnsen, H. & Llinás, R. Electrophysiological properties of guinea-pig thalamic neurones: an in vitro study. *J Physiol* **349**, 205–226 (1984).
4. Jahnsen, H. & Llinás, R. Electrophysiological properties of guinea-pig thalamic neurones: an in vitro study. *J Physiol* **349**, 205–226 (1984).
5. Suzuki, S. & Rogawski, M. A. T-type calcium channels mediate the transition between tonic and phasic firing in thalamic neurons. *Proc Natl Acad Sci U S A* **86**, 7228–7232 (1989).
6. Perez-Reyes, E. Molecular Physiology of Low-Voltage-Activated T-type Calcium Channels. *Physiological Reviews* **83**, 117–161 (2003).
7. Alitto, H., Rathbun, D. L., Vandeleest, J. J., Alexander, P. C. & Usrey, W. M. The Augmentation of Retinogeniculate Communication during Thalamic Burst Mode. *J Neurosci* **39**, 5697–5710 (2019).
8. Borden, P. Y. *et al.* Thalamic bursting and the role of timing and synchrony in thalamocortical signaling in the awake mouse. *Neuron* **110**, 2836-2853.e8 (2022).
9. Crick, F. Function of the thalamic reticular complex: the searchlight hypothesis. *Proc Natl Acad Sci U S A* **81**, 4586–4590 (1984).
10. Reinagel, P., Godwin, D., Sherman, S. M. & Koch, C. Encoding of Visual Information by LGN Bursts. *Journal of Neurophysiology* **81**, 2558–2569 (1999).

11. Sherman, S. M. A wake-up call from the thalamus. *Nat Neurosci* **4**, 344–346 (2001).

12. Swadlow, H. A. & Gusev, A. G. The impact of 'bursting' thalamic impulses at a neocortical synapse. *Nat Neurosci* **4**, 402–408 (2001).

13. Carmody, D. P. & Lewis, M. Brain activation when hearing one's own and others' names. *Brain Res* **1116**, 153–158 (2006).

14. Lepistö, T. *et al.* Auditory stream segregation in children with Asperger syndrome. *Biol Psychol* **82**, 301–307 (2009).

15. Koldewyn, K., Whitney, D. & Rivera, S. M. The psychophysics of visual motion and global form processing in autism. *Brain* **133**, 599–610 (2010).

16. Miller, M. *et al.* Response to Name in Infants Developing Autism Spectrum Disorder: A Prospective Study. *J Pediatr* **183**, 141-146.e1 (2017).

17. Schwartz, S., Wang, L., Shinn-Cunningham, B. G. & Tager-Flusberg, H. Neural Evidence for Speech Processing Deficits During a Cocktail Party Scenario in Minimally and Low Verbal Adolescents and Young Adults with Autism. *Autism Res* **13**, 1828–1842 (2020).

18. Stantić, M., Ichijo, E., Catmur, C. & Bird, G. Face memory and face perception in autism. *Autism* **26**, 276–280 (2022).

19. Moore, D. J. Acute pain experience in individuals with autism spectrum disorders: A review. *Autism* **19**, 387–399 (2015).

20. Lucker, J. R. & Doman, A. Neural Mechanisms Involved in Hypersensitive Hearing: Helping Children with ASD Who Are Overly Sensitive to Sounds. *Autism Research and Treatment* **2015**, 369035 (2015).

21. Takarae, Y., Sablich, S. R., White, S. P. & Sweeney, J. A. Neurophysiological hyperresponsivity to sensory input in autism spectrum disorders. *J Neurodevelop Disord* **8**, 29 (2016).

22. Mikkelsen, M., Wodka, E. L., Mostofsky, S. H. & Puts, N. A. J. Autism spectrum disorder in the scope of tactile processing. *Developmental Cognitive Neuroscience* **29**, 140–150 (2018).

23. Santoro, M. R., Bray, S. M. & Warren, S. T. Molecular mechanisms of fragile X syndrome: a twenty-year perspective. *Annu Rev Pathol* **7**, 219–245 (2012).

24. Jun, J. J. *et al.* Fully Integrated Silicon Probes for High-Density Recording of Neural Activity. *Nature* **551**, 232–236 (2017).

25. Grubb, M. S. & Thompson, I. D. Visual response properties of burst and tonic firing in the mouse dorsal lateral geniculate nucleus. *J Neurophysiol* **93**, 3224–3247 (2005).

26. McCormick, D. A. & Pape, H. C. Properties of a hyperpolarization-activated cation current and its role in rhythmic oscillation in thalamic relay neurones. *J Physiol* **431**, 291–318 (1990).

27. Destexhe, A. & Sejnowski, T. J. Interactions between membrane conductances underlying thalamocortical slow-wave oscillations. *Physiol Rev* **83**, 1401–1453 (2003).

28. Destexhe, A., Mainen, Z. F., Sejnowski, T. J., Koch, C. (EDITOR) & Segev, I. (EDITOR). Kinetic Models of Synaptic Transmission.

29. Huguenard, J. R. Low-threshold calcium currents in central nervous system neurons. *Annu Rev Physiol* **58**, 329–348 (1996).

30. Sherman, S. M. & Guillery, R. W. The role of the thalamus in the flow of information to the cortex. *Philos Trans R Soc Lond B Biol Sci* **357**, 1695–1708 (2002).

31. Halassa, M. M. *et al.* Selective optical drive of thalamic reticular nucleus generates thalamic bursts & cortical spindles. *Nat Neurosci* **14**, 1118–1120 (2011).

32. Sincich, L. C., Adams, D. L., Economides, J. R. & Horton, J. C. Transmission of Spike Trains at the Retinogeniculate Synapse. *J Neurosci* **27**, 2683–2692 (2007).

33. Pachitariu, M., Sridhar, S. & Stringer, C. Solving the spike sorting problem with Kilosort. 2023.01.07.523036 Preprint at https://doi.org/10.1101/2023.01.07.523036 (2023).

34. Rhim, I., Coello-Reyes, G. & Nauhaus, I. Variations in photoreceptor throughput to mouse visual cortex and the unique effects on tuning. *Sci Rep* **11**, 11937 (2021).

35. Kalmbach, B. E., Johnston, D. & Brager, D. H. Cell-Type Specific Channelopathies in the Prefrontal Cortex of the fmr1-/y Mouse Model of Fragile X Syndrome. *eNeuro* **2**, (2015).

36. Routh, B. N. *et al.* Increased transient Na+ conductance and action potential output in layer 2/3 prefrontal cortex neurons of the fmr1-/y mouse. *J Physiol* **595**, 4431–4448 (2017).